The Structural Changes of Gluten/Glycerol Plastics at Dry and Moist Conditions and during Tensile Tests

Shun Yu[1,], Fei Chen[1], Qiong Wu[1], Stephan V. Roth[1,2], Karsten Brüning[3], Konrad Schneider[4], Ramune Kuktaite[5], Mikael Hedenqvist[1]*

1 Department of Fiber and polymer technology, Royal Institute of Technology, Teknikringen SE-10044, Stockholm, Sweden

2 Photon Science, Deutsches Elektronen-Synchrotron (DESY), Notkestraße 85, D-22607 Hamburg, Germany

3 Stanford Synchrotron Radiation Lightsource, Stanford University, 2575 Sand Hill Rd. MS 69, Menlo Park, CA 94025, USA

4 Leibniz-Institut für Polymerforschung Dresden e.V., Mechanik und Struktur, Hohe Straße 6, D-01069 Dresden, Germany

5 Department of Plant Breeding, the Swedish University of Agricultural Sciences, SE-230 53 Alnarp, Sweden

[*] Corresponding Author: E-mail: shuny@kth.se (S.Y.)

ABSTRACT

The structures of wheat gluten based materials are greatly influenced by plasticizer content, moisture content and external mechanical loading. In this study, the effects of moisture on the structure of wheat gluten (WG) plasticized by glycerol was investigated by using in situ small/wide angle x-ray scattering (SAXS/WAXS), mechanical tensile testing and thermal analyses. The materials were processed with additives of ammonium hydroxide/salicylic acid or urea and conditioned at 0, 50 and 100 % relative humidity (RH). In general, water showed similar effects on the WG structure and mechanical properties regardless of the type of additive. It was observed that the known hexagonal close-packed (HCP) structure in WG was present mainly in moist conditions and swelled with the increasing water content. The absorbed water molecules hydrated the protein chains at 50% relative humidity and further led to the formation of a separate water/glycerol phase at 100% relative humidity. An interesting feature was observed by in situ SAXS during the tensile deformation, both the HCP structure and other protein aggregates packed more densely in both the tensile and transverse directions. It is interpreted as that "randomly oriented" chains were drawn out and stretched in the tensile direction, which squeezes the self-assembled structures together, similar to "tightening a knot".

KEYWORDS:

Wheat gluten, Relative humidity, X-ray scattering, Hexagonal close-packed structure, Hydration

Introduction

The increasing pressure on petroleum based materials in terms of available resources and price drives need to look for alternatives. Bio-based polymeric materials are one option. They can be directly obtained from sustainable resources, such as, plants, or from the industrial processing of the plants, for example, as a byproduct from bioethanol production. Meanwhile, plant proteins, such as wheat gluten (WG), zein, and soybean protein, are readily available at a low-price[1]. Extensive investigations have enabled future use of bio-based polymeric materials in different applications[1]. For example, WG has been converted into useful engineering plastics with the good barrier properties[2–4], flame retardation function[5], foam properties[6], environmental purification properties[7] and mechanical properties[8–10]. WG-based composites have also shown the potential as a substitute of synthetic polymers in packaging and construction areas.[11,12]

To further improve WG mechanical properties, optimal thermo-mechanical processing and the full understanding of the effects of moisture content are critical.[13,14] On one hand, the wheat gluten without plasticizer becomes brittle and difficult to handle[4]. Hence, a plasticizer is needed to lower the melt-viscosity during the processing of WG and improve the toughness of the final product.[15] On the other hand, if WG contains too high plasticizer content, the plasticizer-polymer interactions dominates over polymer-polymer interactions, resulting in poor strength and barrier properties[16,17] Wheat gluten proteins are hydrophilic, which requires that the plasticizers are also hydrophilic, like glycerol and sorbitol. Since water also plasticizes WG, it is important to control the moisture content of the WG materials with or without an additional plasticizer to prevent inferior properties. Hernández-Muñoz et al.[18], have shown that addition of glycerol increases the moisture absorption of WG. In their work, the moisture sorption isotherms of WG with glycerol were reported to follow a sigmoidal shape – the equilibrium moisture content of materials increased slowly up to 65 % relative humidity (RH) and then rapidly rose by further increase in RH. In order to lower the water uptake and permeability of wheat gluten materials, one way is to add hydrophobic additives[19,20]. Another way is to avoid using a plasticizer, which requires that WG is strengthened, for example, by adding macromolecular-crosslinkers into WG[9,10,21–23]. Despite some

successful strategies against increasing water permeability, the effects of water on the hierarchical structure of WG are still not clear[24].

The structure of the WG protein is only partially understood because of its complexity.[25] WG is a protein blend consisting of two main components: gliadin (monomeric protein) and glutenin (polymeric protein). Gliadin contributes mainly to the viscous behavior of the material, while glutenin influences mainly the elasticity[18,26]. Typically, the pristine WG has no regular self-assembled structure, but denatured aggregates can develop at an elevated temperature, especially in the presence of glycerol.[25] Further thermal treatments can even generate hexagonal close-packed nanostructures (HCP) in WG platics.[25,27,28] Besides the plasticizers, additives, such as acids, bases and urea, have been used to improve the processability of WG.[26,29–31] Interestingly, new tetragonal-packed and HCP nanostructures were discovered in the WG with NaOH and ammonium hydroxide (AH)[28]. A similar HCP structure was also reported in the presence of urea, which act as a combined protein denaturant and plasticizer.[32] In spite of the discovery of various self-assembled structures, the study on their detailed structure and function is still ongoing and the effects of moisture content on those have not been clearly elucidated. Furthermore, how these structures change during mechanical deformation under different RH conditions is still unknown. It is thus important to clarify these issues for the reliable use of WG in a number of applications, especially for extruded films and injection molded items.[33]

In this work, we have combined in-situ small and wide angle x-ray scattering (SAXS/WAXS) techniques with tensile testing to monitor the WG structural changes on a molecular level at different moisture contents. Extruded glycerol-plasticized WG films, prepared by the addition of ammonium hydroxide/salicylic acid and urea, were selected since they have shown interesting processability, mechanical properties and material structures, as well as their potential for commercial exploitation[32,34]. Three RH conditions (RH0, RH50 and RH100) were chosen in order to work with systems with clear variations in structure and properties. Together with differential scanning calorimetry (DSC) and cyclic tensile tests, the structural and mechanical changes due to variations in moisture content were determined.

Experiments

Materials and Sample Preparation

The preparation of the samples has been described in full detail elsewhere[32,34], and is therefore only briefly described here. The pristine wheat gluten powder was provided by Lantmännen Reppe AB Sweden (77.7% dry weight of gluten protein). Before extrusion, the WG was conditioned, mixed with glycerol plasticizer (WG:glycerol ratio: 7:3) and further prepared with ammonium hydroxide (AH) together with salicylic acid (SA) or urea (U) to improve the processability and final properties.[31,32,34] Unless specifically mentioned, the term WG hereinafter refers to WG mixed with glycerol. The AH contents were 3, 5 and 10 %, all with 1.5 % of salicylic acid[30,31] (% refers to the total weight (WG + glycerol + AH/SA)) and the urea contents were 10, 15 and 20 % (% refers to the total weight (WG + glycerol + urea)). The samples were named accordingly as AHx (including SA) and Uy, where x and y are the contents. The materials were extruded in an Axon BX12 single-screw extruder with a slit sheet die into films with a thickness of ca. 1 mm and a die temperature of 130 ˚C (urea) or 130-140 ˚C (AH). Dumb-bell shaped specimens with a total length of 40 mm were punched from the film for the tensile tests. The width and length of the narrow section were 3 mm and 6.2 mm, respectively. The specimens were divided into 3 groups for the moisture conditioning in desiccators with silica gel, saturated $Mg(NO_3)_2$ aqueous solution and pure milli-Q water. The relative humidity (RH) in these cases were close to 0, 54[35] and 100 % at room temperature. The three conditions were denoted RH0, RH50 and RH100, respectively. The sample conditioning time prior to tensile testing was at least 72 h. The dry weight content of materials is evaluated by the dry weight percentage $\eta = \frac{w_0}{w_x} \times 100\ \%$, where w_0 is the sample weight at RH0 and w_x is the sample weight in equilibrium with a relative humidity of x %. Then moisture content is calculated as 100-η (%).

Experimental Methods

The X-ray scattering characterization was carried out at the P03 “MiNaXS” beamline at PETRA III storage ring, Deutsches Elektronen-Synchrotron (DESY), Hamburg.[36,37] A home-made tensile rig was

used to carry out both mechanical deformation and small/wide angle X-ray scattering[38,39]. The tensile rig was mounted on top of a hexapod for fine sample alignment. The two tensile heads move in opposite directions at a speed of 0.05 mm/s, which corresponds to 0.1 mm/s displacement rate. The length of the specimen between the clamps is approximately 6 mm before deformation and the strain rate is 100 % /min. The Pilatus 1M detector was used for the SAXS measurement with a sample-to-detector distance (SDD) of 2134.3 ± 0.1 mm. The Pilatus 300k detector was used for the wide angle X-ray scattering (SAXS) with an SDD of 92.3 ± 0.1 mm. The X-ray wavelength was 0.957 Å. The exposure time for both SAXS and WAXS was 1 s/frame. Beam damage was carefully checked by monitoring the scattering intensity change as a function of continuous X-ray exposure at a single spot and minimized by scanning each specimen in small steps during the tensile test. Before each measurement, the specimen was rapidly transferred to the measurement stage in the experimental hutch at room temperature with ~ 30% RH. The entire characterization process took no more than 10 min, including sample mounting, alignment and measurement. For the data processing, the DPDAK freeware was used[40]. SAXS patterns were processed with Lorentz correction (I(q) times q^2 for the correction of 3D to 2D projection) and plotted as a Kratky plot: $I(q)q^2$ versus q.

Differential scanning calorimetry (DSC) measurement was carried out on selected AH5 and U15 samples stored at RH0, RH50 and RH100. The sample was cooled to -50 °C from 25 °C with a cooling rate of 10 °C/min. After 3 min at -50 °C the sample was heated to 150 °C with a heating rate of 10 °C/min. The sample weight was 14 mg ± 2 mg. Cyclic tensile tests were carried with the Instron 5944 tensile tester in an environmental controlled room (50±2 % RH and 23±1 °C). The specimens were punched out from the films into dumb-bell shapes with a width and length of the narrow deformation region of 4 mm and 20 mm, respectively. The strain rate was 100 %/min with respect to the original length in both loading and unloading. The cycles were designed to stretch the samples till 2, 5, 10, 20, 40, 60, 100 and 300 % during the sequential cycles and were unloaded till zero stress before the subsequent cycle started. Conditioned samples at RH0 and RH100 were transferred from the desiccators to the measuring stage right before the measurement.

Results and Discussion

Table 1. shows the moisture content of samples stored at different RHs. Moisture content in the dry samples conditioned at RH0 is zero. The samples exposed to RH50 contain around 10 % moisture content. A dramatic increase of moisture content was found for the samples conditioned at RH100 by more than 50%. Nevertheless, the moisture uptake was essentially independent of the AH and urea contents, with the exception of the greater water uptake with higher urea content at RH 100.

Table 1 moisture content in WG at different RH

Relative humidity [%]	Moisture content [%]					
	AH3	AH5	AH10	U10	U15	U20
0	0	0	0	0	0	0
50	9.5	9.3	9.4	10.4	10.8	11.0
100	51.6	51.0	51.4	55.6	57.5	58.9

Figure 1 shows the WAXS profile of WG with (a) AH and (b) urea at different RH conditions. In all cases, the dry sample had a small hump (d_1) and a dominant peak (d_2), in agreement with previous reports.[25,27] No sharp Bragg peak was observed in any of the samples under any conditions, indicating that the WG structure was amorphous. The real space distances were estimated according to the equation: $d = 2\pi/q$, where q is the length of the reciprocal lattice vector. This yielded a d_1 value of 0.96 nm for all samples, independent of relative humidity. However, this result should be treated with care since the humps were very small and changes in d_1 with e.g. moisture content may be difficult to observe. It has been suggested that d_1 is the distance between neighboring α–helices.[25,41] It was previously suggested that the low intensity of d_1 was due to the addition of glycerol.[25] At RH0, d_2 for AH-WG was 0.44 nm, while for Urea-WG, this peak appeared at a slightly higher q value and a shorter distance: d_2=0.42 nm. These values, being independent of AH and urea content, are close to the typical interchain distances of amorphous polymers.[42] Naturally, the intensity in this region may be also convoluted with the contributions from

protein intrachain, as well as additive-protein distances. It is interesting to note that the samples with urea had a smaller d_2 value than the AH samples, despite the generally higher content of urea added (urea also remains in the sample while AH evaporates). Kuktaite et al.[27] reported that the increase of the urea concentration can lead to more compact protein polymeric structures. The shorter d_2 with urea may indicate that urea promotes a more extensive denaturation of the protein and consequently the protein chains aggregates more densely.[43] With increasing moisture content a new broad scattering feature at higher q values developed (~ 17.0 nm^{-1}), corresponding to a distance of d_{water} = 0.37 nm. As expected the relative intensity of the d_2-peak became smaller with increasing water content, however, the position of d_2 appeared to not change. The absence of the expected increase in d_2 (decrease in q) due to a swelling structure was a consequence of the overlapping d_2 and d_{water} intensities. The very broad nature of this peak made it impossible to separate the two contributions in a meaningful way by curve deconvolution. One possible origin of this peak can be attributed to the hydrated protein structure. As mentioned above, for typical amorphous polymers, the amorphous structures lead to a scattering feature (halo) with a maximum at an inter-chain distance of ca. 0.4 nm.[42] Evidently the moisture-induced feature did not match the value of the halo. It is known for salts-containing gluten proteins that the ionic additives facilitate the exposure of polar and ionic groups of the protein at the surface and promote the interaction of protein with water molecules via hydration.[44] Another possible origin of this peak is water molecule aggregates in the protein system. The ionic interaction (protein-salt-protein) may help the formation of hydrophilic networks where water molecules aggregate and form micro-droplets in the hydrated protein matrix.[44,45] In this case, the d_{water} position was close to reported intermolecular distances of water clusters in water containing polymeric materials.[46–48] Furthermore, in our samples, there is a large amount of glycerol besides the AH and urea. Glycerol also interacts with water and the glycerol-water mixture may show different X-ray diffraction peak position depending on the concentration.[49]

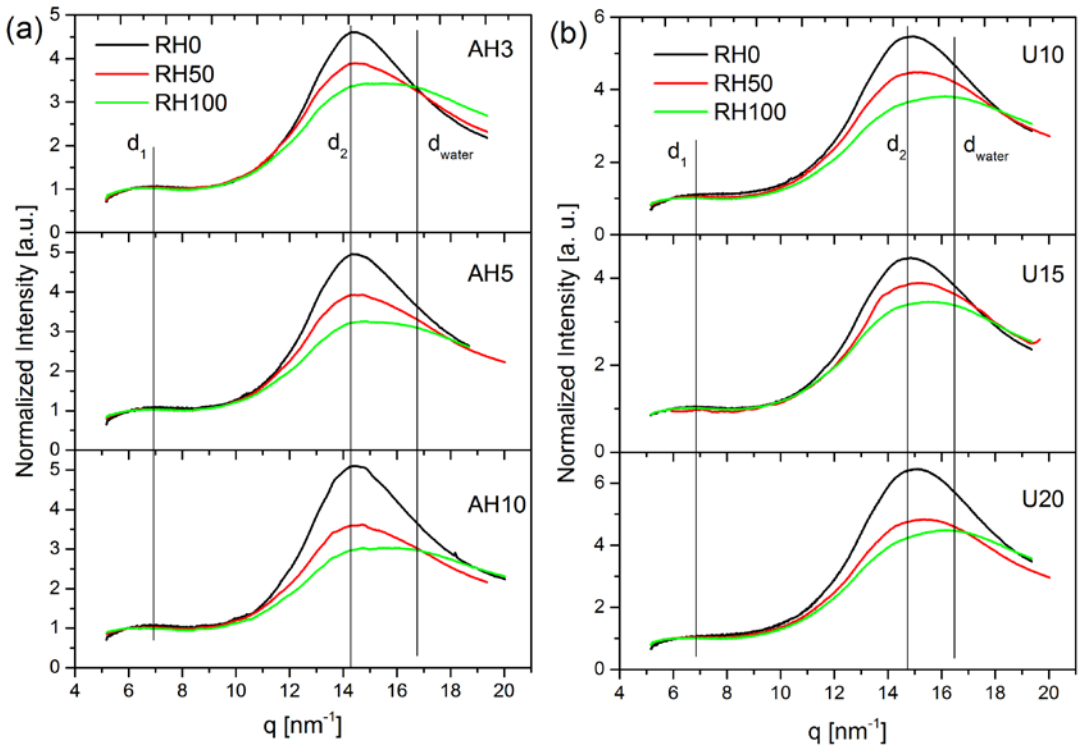

Figure 1. WAXS of pristine WG with (a) AH and (b) urea at different relative humidities as a function of the length of the reciprocal lattice vector (q). The vertical lines mark the features d_1 and d_2 related to WG, and a feature due to water, d_{water}.

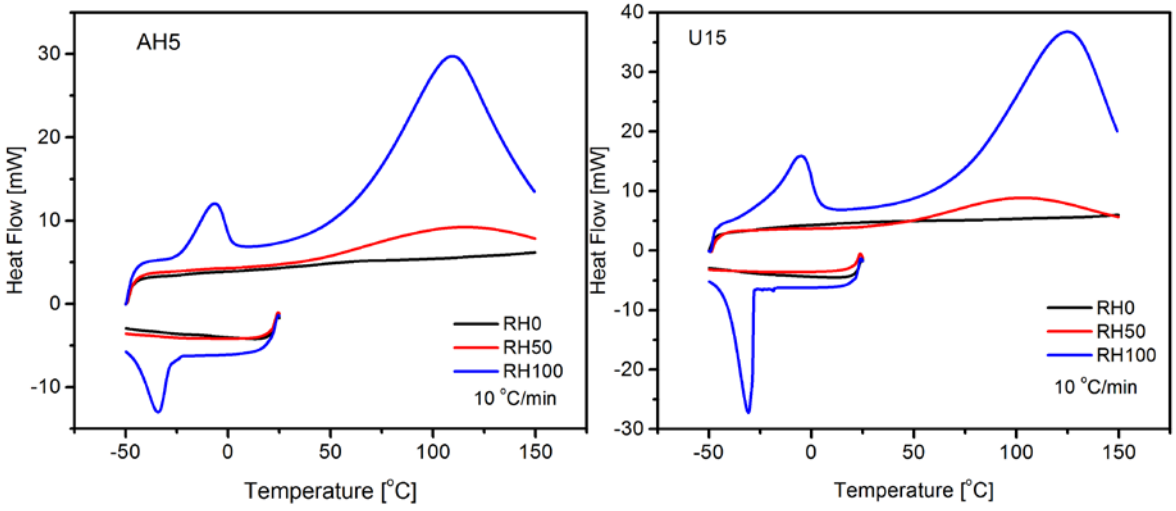

Figure 2. DSC diagram of AH5 and U15 obtained in temperature ramping cycles: cooling path from room temperature to -50 °C and heating path from -50 °C to 150 °C.

For deeper insight regarding the origin of d_{water}, DSC measurements were performed on selected samples (AH5 and U15) because all samples showed similar trends in WAXS. The results are summarized in Figure 2. First of all, DSC showed similar features for both samples. The samples exposed to RH 0 and RH 50 did not show any obvious difference in the cooling curve and the heating curve below room temperature. No crystallization of ice was observed. However, a broad endothermal peak appeared for the RH50 samples peaking at ca. 100 °C or above. It corresponded to the evaporation of water or water-rich (glycerol/urea) mixtures. The absence of ice crystallization for the samples conditioned at RH50 indicates that d_{water} was mainly due to a hydrated protein structure. For the samples exposed to RH 100, a clear endothermal peak was observed at ca. -30 ^{o}C during cooling and an exothermal peak appeared around -10 ^{o}C during heating for both AH5 and U15, with only subtle peak shift. The crystallization and melting peaks indicate that water is forming a separate phase in the WG material at RH100 besides hydrating the protein chains. The fact that the crystallization and melting points are lower than those of pure water suggests that the separate phase is a water mixture with glycerol and in the case of U15 possibly also urea. The freezing point of a water solution with a high content of urea (8 mol/kg (52 wt.%) urea) shows a depression of 11.4 °C[50], which is still far from the actual depression. In addition, since both the AH and urea systems behave similar, the additives (AH, salicylic acid and urea) did not seem to play a major role for the formation of the separate water phase. However, the freezing point of a glycerol-water mixture with ca. 60 % glycerol and 40 % water coincide with the present DSC peak[51]. Hence, it is plausible to assume that at RH100, the separate water phase contained a sizeable amount of glycerol. Thus, d_{water} can be ascribed to two main contributions: hydrated protein and a glycerol/water phase (possibly with also urea in the urea samples). As expected the evaporation peaks in the RH100 systems were larger than that in the RH50 systems with a boiling point somewhere between 100 and 125 °C.

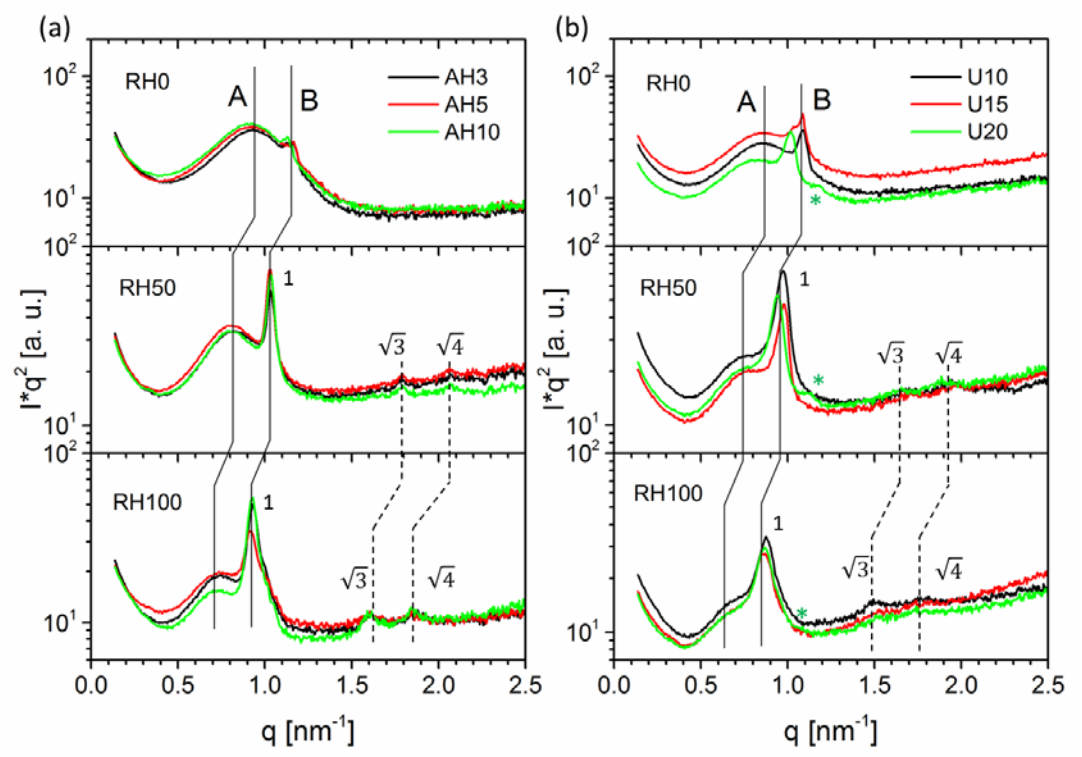

Figure 3. Kratky plot ($I \times q^2$ $vs.$ q) of SAXS data on pristine WG with (a) AH and (b) urea at different RHs. The reflections of the HCP structure are labeled as 1, $\sqrt{3}$ and $\sqrt{4}$. Green (*) signs in Urea-WG indicate a satellite feature.

The Kratky plots of the SAXS data of WG with AH and urea are shown in Figure 3. SAXS reveals the structure on the nanoscale. Two features, marked A and B, are clearly observable at all RH levels. A is a broad peak typically observed for WG with glycerol, and it is suggested to originate from the structure of aggregates after the denaturation of the protein. It mainly involves proteins with a large amount of disulphide and irreversible bonds.[25,52] The sharper B peak at higher q values indicates a correlated packing of the materials structures, which is perhaps related to the first order reflection of the HCP nanostructure packing of WG in the presence of glycerol and additives.[28,52] It was previously reported that a similar structure exists in gliadin mixed with glycerol.[25] The size of the HCP structure has been shown to vary with both temperature and additives present, for instance, it increases in the presence of urea.[52] In the present case, a similar trend was found for WG with urea at RH0 and RH50; the peak for U20 being at a

lower q value than those for U10 and U15. A small peak, marked (*), occurred after the first order reflection of the HCP structure of U20 at all RH levels. This peak has been reported by Kuktaite et al.[27] and has been assigned to a structure with a large amount of hydrogen bonds between the protein and the urea.

The moisture-induced structural change was quite consistent for both AH-WG and urea-WG. At RH0, only A and B were observed for both materials and no higher order reflections of the HCP structure were found. Nevertheless, peak B was more dominant in the urea-WG curves than in the AH-WG curves. As the relative humidity increased, both A and B shifted towards the smaller q value. As the real space distance is $d = 2\pi/q$, such shift indicates a moisture-induced expansion of the structure. With increasing RH, feature B clearly evolved into the first order reflection of the HCP structure with pronounced higher order reflections marked as $\sqrt{3}$ and $\sqrt{4}$. Such a structural evolution with increasing moisture content indicates that water actually takes part in establishing the WG nanostructures. Additionally, the ratio between the integrated peak area of the HCP related structures (Peak B or HCP) and that of large aggregates (Peak A) also increased with increasing RH (see support information Figure S1). This indicated that the HCP structures are more favorable than the large aggregates at higher RH.

By combining both SAXS/WAXS and DSC, the RH-dependent structural evolution is summarized as a molecular structure model in Schematic 1. At RH0, the aggregates were closely packed, and the HCP components were squeezed so tight that there was little correlation between the components in the materials and there was no pronounced higher order packing as observed in SAXS. At RH 50, the aggregated structures expand by absorbing water via hydration. Meanwhile, the HCP components also become mobile and form stable HCP structures with a correlated distance, probably via hydrogen bonds introduced by the water. It is shown as the higher order reflections in SAXS. Glycerol is still molecularly dissolved in the protein matrix at RH0 and RH50. At RH100, both the aggregates and HCP structure are expanded via extensive hydration. Additionally, part of the glycerol molecules mix with abundant water, forming a separate phase together.

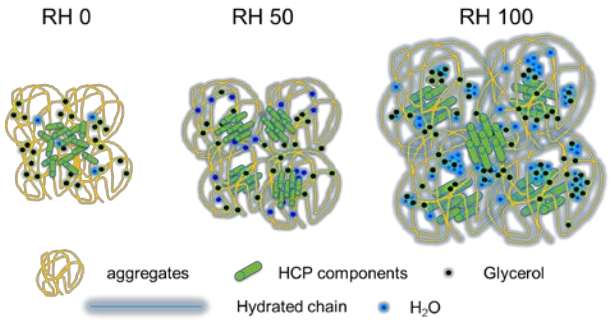

Schematic 1. The influence of moistures on the WG structure

In Figure 4, AH5 and U15 have been selected to illustrate the results of the combined tensile testing and in-situ SAXS. The mechanical properties of all samples are summarized in Table S1 in the support information. As observed here and in the Table S1, the modulus and strength decreased with increasing moisture content for all samples. The trend in the strain at break was less conclusive. However, considering the whole range in RH, it seems that the samples fractured at lower strain at 100% RH than at 0% RH. The strength values showed that the materials were weakest at 100% RH. The 2D SAXS data show a clear reorientation of the material during the tensile test. The isotropically distributed intensity close to the central beam became anisotropic with stronger intensity perpendicular to the strain direction, and the intensity of the sharper outer ring (peak B in Figure 3) followed a similar trend. However, the ring structure in the strain direction could still be observed even just before the samples broke, indicating that the re-orientation of the scattering objects to the strain direction was not complete when fracture occurred. It should be noted that some of the specimens showed a slight orientation prior to the tensile test, originating from the extrusion.[28] Nevertheless, this pre-orientation did not affect the general conclusions regarding the effects on the material structure of the uniaxial tensile deformation.

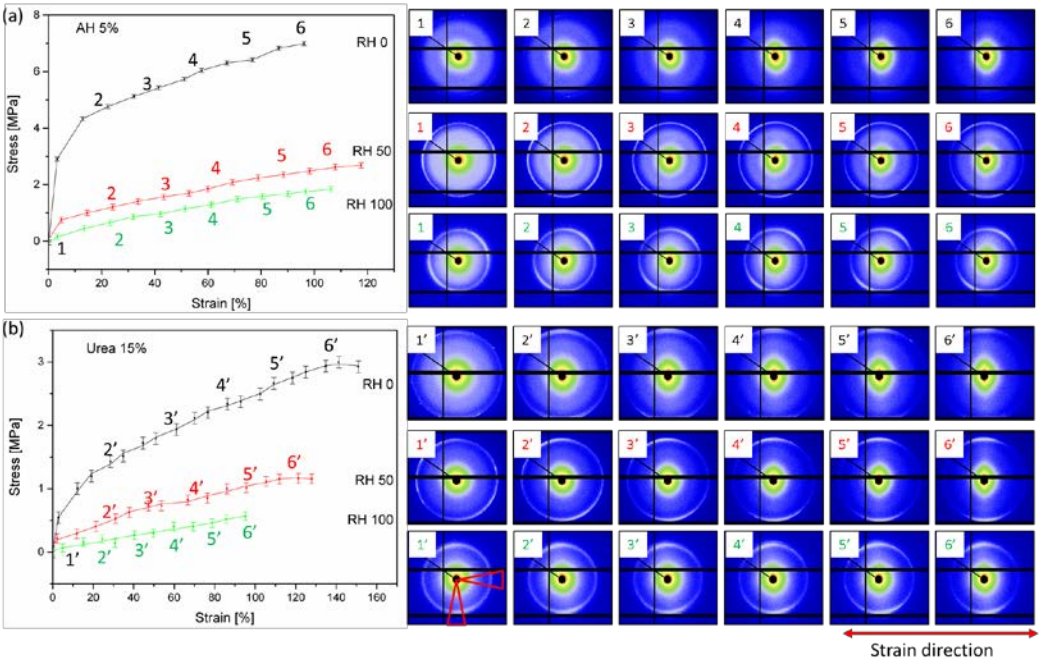

Figure 4. Stress vs. strain of AH5 and U15 (left panel) and the corresponding 2D SAXS patterns at the marked positions (right panel). The red triangles in the bottom row mark the parallel-cut and perpendicular-cut integration area for further analyses in Figure 5.

Figure 5 shows the Kratky plot of the SAXS data of all samples extracted from the directions parallel and perpendicular to the strain direction. For AH-WG, at RH0 (Figures 5a and b, first row), the broad peak related to the WG aggregates (peak A in Figure 3) shifted gradually to larger q values in both the parallel and perpendicular directions with increasing the strain. At the same time, the intensity of this peak decreased in both directions. This indicated that the aggregated structures became fewer and smaller during the deformation, possibly because the uniaxial loading broke the bonds within the aggregates by pulling chains apart so that the harder "cores" were squeezed tighter or even disappeared (like "opening a bow"). The small peak at higher q (peak B in Figure 3) showed a similar trend during the mechanical deformation. At RH50 (Figures 5a and b, second row), the initial positions of peaks A and B were located at lower q values than at RH0, indicating swollen structures. As the strain increased, the intensities of both peaks decreased along the parallel cut, especially for peak B, whereas the intensities became more

intense in the perpendicular cut. Meanwhile, the peak B shifted towards the larger q value (0.02 nm^{-1}), corresponding to a shrinkage of 0.12 nm in real space. This suggests that the HCP structures were aligned to a greater extent with the strain direction during tensile deformation, and that they became more compact due to the local stress. At RH100, an additional peak appeared at ca. 1 nm^{-1} in all the AH-WG samples (Figure 5b, row 3). A similar peak was previously observed in WG with 20 % urea and was assigned to the structure induced by a large amount of hydrogen bonds between the protein and urea.[52] Since no urea is present in AH-WG, this peak should then be associated to a large amount of hydrogen bonds mediated via the water and glycerol molecules, and the ionic interaction induced by the salt ingredients (although there is likely very little ammonium hydroxide left in the sample after the processing step). As the strain increased, the evolution of this peak intensity and position is similar to those at RH50.

The Kratky plots of urea-WG during the tensile test are shown in Figures 5c and d. In all cases, a clear and sharp peak B was observed. As aforementioned, this peak is related to the first order of the HCP structure, which can be formed in WG by addition of urea.[52] As the strain increased, this peak shifted towards higher q values in both the parallel and perpendicular directions, while the peak intensities decreased in the parallel direction and increased in the perpendicular direction. The explanation is, as mentioned above, that the WG nanostructure became more compact because of the “opening the bow” phenomenon and the HCP objects aligned along the strain direction.

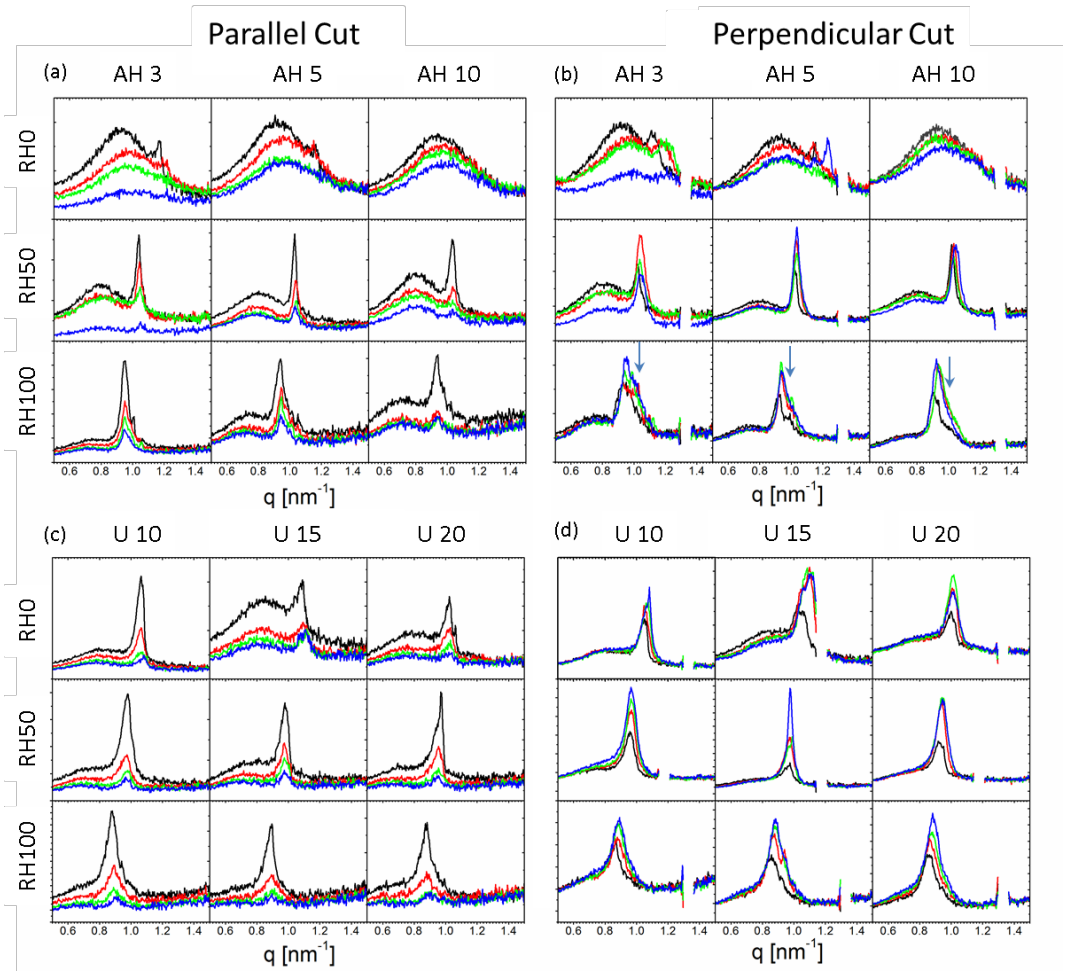

Figure 5. Kratky plot of the SAXS data ($I \times q^2$ *vs.* q) parallel and perpendicular to the strain direction during the tensile test. The integration areas along the two directions in each case are marked in Figure 4. The colors of the curve marks the strain relative to the strain immediately before the sample broke: black (0%), red (33%). green (66%) and blue (~ 100%). The arrows in (b) mark the additional feature developed at high moisture content.

To further distinguish the elastic and non-elastic contribution to the mechanical deformation of the WG material, we choose again AH5 and U15 to carry out cyclic tensile tests. Figure 6a and b show the cyclic tensile curves for AH5 and U15, respectively. The clear hysteresis is observable between the loading and unloading parts, which originate from energy losses in the materials during the cyclic loading. In each cycle, the materials were unloaded till zero stress after the target strain was reached. The strain corresponds to the zero stress (ε_x) is plotted as a function of the increasing maximum strain in each cycle

(Figures 6c and d). As observed, ε_x increases slower (smaller slope) with increasing water content in the material (slope: RH100<RH50<RH0) for both the AH and the urea systems. This shows that the elastic contribution to the tensile deformation increased with increasing water content and/or that the time-dependent elastic strain recovery was faster in the presence of higher water content. In figure 6e and f, the relative changes of the modulus calculated from the initial slope of each loading part of the cycle have been compared. Interestingly, for all samples, the modulus went through a maximum, which occurred mainly for the cycle with the maximum strain of 5%. We can only speculate about the reason for this behavior. An increase in modulus can arise from a gradual orientation of the polymer chains in the tensile direction; however, this would be expected to be stronger at larger strains, where we instead observed a decrease in modulus. The decrease in stiffness at larger strains was not accompanied by a weaker structure, the strength was not reduced with increasing number of cycles (Figures 6a and b) Nevertheless, a cycle-induced softening always occurred which dominated over orientation-effects at larger strains (Figure 6e and f).

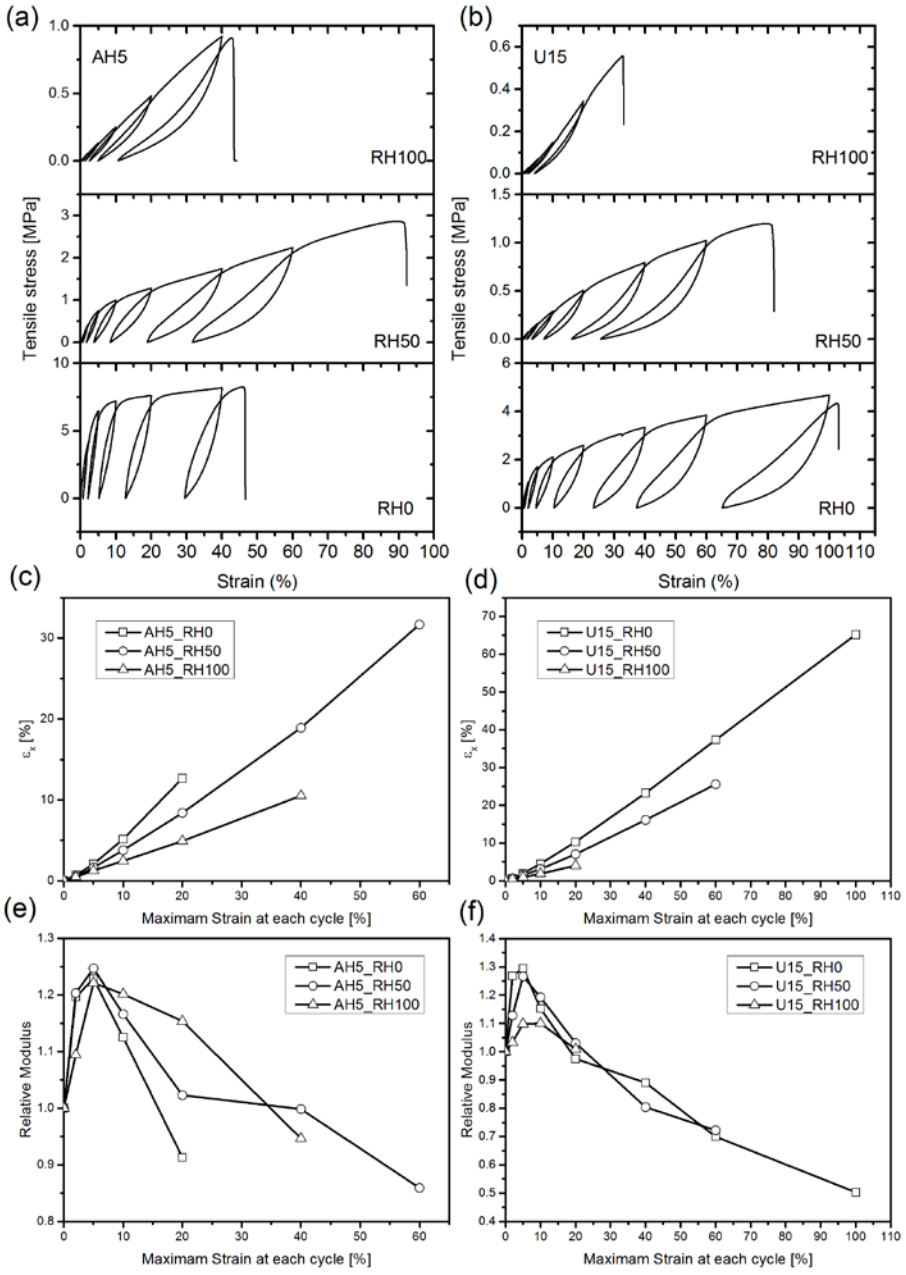

Figure 6. Cyclic tensile tests on AH5 (a) and U15 (b) at RH0, RH50 and RH100. (c) and (d) are the strain corresponds to the zero stress (ε_x) as a function of that maximum strain of each cycle; the relative modulus of AH5 (e) and U15 (f) are extracted from the initial rising slope at each cycle and are plotted against the maximum strain of each cycle. The status of zero maximum strain at each cycle is defined as the first rising stretching from 0 to 2% strain. The corresponding ε_x at zero maximum strain at each cycle is zero and the modulus at zero maximum strain is also extracted from the first rising slope.

The effects of uniaxial tensile deformation on the WG materials are summarized in Schematic 2. For both AH-WG and urea-WG at RH0, few ordered structures were present in the bulk materials. During deformation, sections of the protein aggregates were pulled apart and, at the same time, more compact regions were formed with more densely-packed entangled chains. It was observed as an intensity decrease of peak A at RH0, both parallel and perpendicular to the strain direction. Meanwhile, the peak shifted towards higher q values. Additionally, structures with a short correlated distance (peak B) were squeezed even closer and some became oriented parallel to the tensile direction. The deformation here was to a large extent non-elastic as shown by the cyclic measurements. For AH-WG and urea-WG at RH50 and RH100, the mechanical deformation aligned HCP structures progressively in the strain direction, as observed by the anisotropic intensity distribution with a significantly higher SAXS intensity in the perpendicular direction. A possible explanation is that the HCP structure was squeezed tighter as a consequence of surrounding chains being stretched in the strain direction.

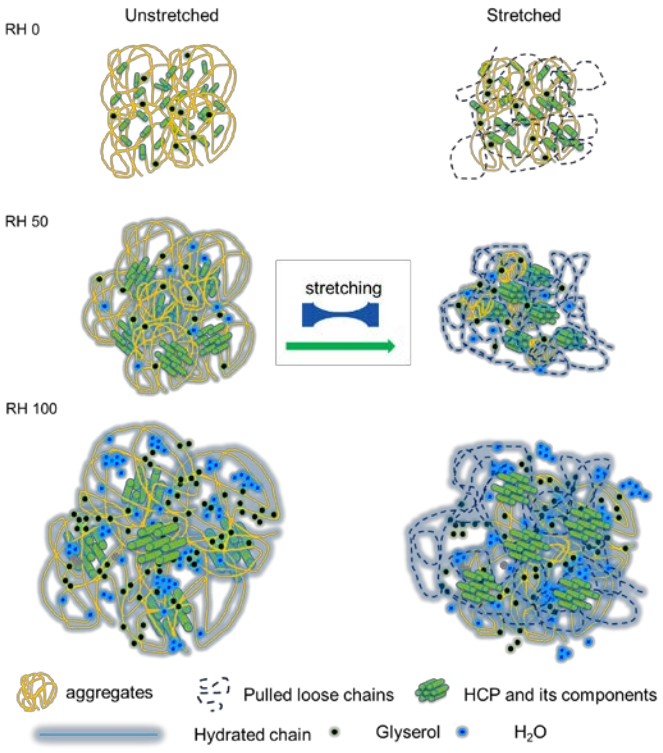

Schematic 2. The structure of WG under uniaxial tensile deformation in dry and moist conditions.

Conclusions

We have investigated the influence of moisture on the structure of WG/glycerol materials produced with ammonium-hydroxide/salicylic acid and urea additives and the corresponding changes in mechanical properties. Both types of materials (AH-WG and urea-WG) contained an HCP superstructure at high RH levels, which was absent or present in only a low amount in dry conditions. Clearly, the presence of moisture, through a large number of hydrogen bonds, stabilized the HCP nanostructure in the WG materials. On the other hand, the formed hydrated protein chains and the phase-separated water/glycerol component decreased the strength of both types of WG. This work reveals the significance of moisture in keeping the features of the amorphous protein structure. During the tensile test, the HCP, as well as the aggregated structures, became more densely packed and more oriented in the strain direction. This is suggested to be associated to a squeezing effect caused by surrounding chains that were pulled or stretched extensively in the strain direction ("tightening a knot effect"). The results in this work show how water can affect the structure of amorphous proteins by forming different complex structures at different relative humidity and how this affects the mechanical behavior.

Acknowledgement

S.Y acknowledges the financial support from the Knut and Alice Wallenberg Foundation. Parts of this research were carried out at the light source PETRA III at DESY, a member of the Helmholtz Association (HGF). We would like to thank the beamline staff for assistance in using the beamline P03. Miss Lisa Hedenqvist is acknowledged for helping with the X-ray data processing, Mr. Dongming Liu for the support on DSC measurement and Dr. Erik Linde for the support on the cyclic tensile measurement.

Supporting Information. The ratio of integrated peak area in Figure 4; the table of summarized mechanical properties. "This material is available free of charge via the Internet at http://pubs.acs.org."

References:

(1) Mekonnen, T.; Mussone, P.; Khalil, H.; Bressler, D. Progress in Bio-Based Plastics and Plasticizing Modifications. *J. Mater. Chem. A* **2013**, *1*, 13379.

(2) Cho, S.-W.; Blomfeldt, T. O. J.; Halonen, H.; Gällstedt, M.; Hedenqvist, M. S. Wheat Gluten-Laminated Paperboard with Improved Moisture Barrier Properties: A New Concept Using a Plasticizer (Glycerol) Containing a Hydrophobic Component (Oleic Acid). *Int. J. Polym. Sci.* **2012**, *2012*, 1–9.

(3) Kuktaite, R.; Türe, H.; Hedenqvist, M. S.; Gällstedt, M.; Plivelic, T. S. Gluten Biopolymer and Nanoclay-Derived Structures in Wheat Gluten-Urea-Clay Composites: Relation to Barrier and Mechanical Properties. *ACS Sustain. Chem. Eng.* **2014**, *2*, 1439–1445.

(4) Gontard, N.; Duchez, C.; Cuq, J.-L.; Guilbert, S. Edible Composite Films of Wheat Gluten and Lipids: Water Vapour Permeability and Other Physical Properties. *Int. J. Food Sci. Technol.* **2007**, *29*, 39–50.

(5) Wu, Q.; Andersson, R. L.; Holgate, T.; Johansson, E.; Gedde, U. W.; Olsson, R. T.; Hedenqvist, M. S. Highly Porous Flame-Retardant and Sustainable Biofoams Based on Wheat Gluten and in Situ Polymerized Silica. *J. Mater. Chem. A* **2014**, *2*, 20996–21009.

(6) Blomfeldt, T. O. J.; Nilsson, F.; Holgate, T.; Xu, J.; Johansson, E.; Hedenqvist, M. S. Thermal Conductivity and Combustion Properties of Wheat Gluten Foams. *ACS Appl. Mater. Interfaces* **2012**, *4*, 1629–1635.

(7) Dhandayuthapani, B.; Mallampati, R.; Sriramulu, D.; Dsouza, R. F.; Valiyaveettil, S. PVA/gluten Hybrid Nanofibers for Removal of Nanoparticles from Water. *ACS Sustain. Chem. Eng.* **2014**, *2*, 1014–1021.

(8) Gällstedt, M.; Mattozzi, A.; Johansson, E.; Hedenqvist, M. S. Transport and Tensile Properties of Compression-Molded Wheat Gluten Films. *Biomacromolecules* **2004**, *5*, 2020–2028.

(9) Diao, C.; Xia, H.; Parnas, R. S. Wheat Gluten Blends with Maleic Anhydride-Functionalized Polyacrylate Cross-Linkers for Improved Properties. *ACS Appl. Mater. Interfaces* **2015**, *7*, 22601–22609.

(10) Woerdeman, D. L.; Veraverbeke, W. S.; Parnas, R. S.; Johnson, D.; Delcour, J. A.; Verpoest, I.; Plummer, C. J. G. Designing New Materials from Wheat Protein. *Biomacromolecules* **2004**, *5*, 1262–1269.

(11) Guo, C.; Zhou, L.; Lv, J. Effects of Expandable Graphite and Modified Ammonium Polyphosphate on the Flame-Retardant and Mechanical Properties of Wood Flour-Polypropylene Composites. *Polym. Polym. Compos.* **2013**, *21*, 449–456.

(12) Zhang, X.; Do, M. D.; Dean, K.; Hoobin, P.; Burgar, I. M. Wheat-Gluten-Based Natural Polymer Nanoparticle Composites. *Biomacromolecules* **2007**, *8*, 345–353.

(13) Mekonnen, T.; Mussone, P.; Alemaskin, K.; Sopkow, L.; Wolodko, J.; Choi, P.; Bressler, D. Biocomposites from Hydrolyzed Waste Proteinaceous Biomass: Mechanical, Thermal and Moisture Absorption Performances. *J. Mater. Chem. A* **2013**, *1*, 13186.

(14) Micard, V.; Belamri, R.; Morel, M. H.; Guilbert, S. Properties of Chemically and Physically Treated Wheat Gluten Films. *J. Agric. Food Chem.* **2000**, *48*, 2948–2953.

(15) Vieira, M. G. A.; Da Silva, M. A.; Dos Santos, L. O.; Beppu, M. M. Natural-Based Plasticizers and Biopolymer Films: A Review. *Eur. Polym. J.* **2011**, *47*, 254–263.

(16) Pouplin, M.; Redl, A.; Gontard, N. Glass Transition of Wheat Gluten Plasticized with Water, Glycerol, or Sorbitol. *J. Agric. Food Chem.* **1999**, *47*, 538–543.

(17) Gontard, N.; Ring, S. Edible Wheat Gluten Film: Influence of Water Content on Glass Transition Temperature. *J. Agric. Food Chem.* **1996**, *44*, 3474–3478.

(18) Hernández-Muñoz, P.; Kanavouras, A.; Ng, P. K. W.; Gavara, R. Development and Characterization of Biodegradable Films Made from Wheat Gluten Protein Fractions. *J. Agric. Food Chem.* **2003**, *51*, 7647–7654.

(19) Song, Y.; Zheng, Q. Improved Tensile Strength of Glycerol-Plasticized Gluten Bioplastic Containing Hydrophobic Liquids. *Bioresour. Technol.* **2008**, *99*, 7665–7671.

(20) Zhang, X.; Do, M. D.; Kurniawan, L.; Qiao, G. G. Wheat Gluten-Based Renewable and Biodegradable Polymer Materials with Enhanced Hydrophobicity by Using Epoxidized Soybean Oil as a Modifier. *Carbohydr. Res.* **2010**, *345*, 2174–2182.

(21) Diao, C.; Xia, H.; Noshadi, I.; Kanjilal, B.; Parnas, R. S. Wheat Gluten Blends with a Macromolecular Cross-Linker for Improved Mechanical Properties and Reduced Water Absorption. *ACS Sustain. Chem. Eng.* **2014**, *2*, 2554–2561.

(22) Jansens, K. J. A.; Lagrain, B.; Rombouts, I.; Brijs, K.; Smet, M.; Delcour, J. A. Effect of Temperature, Time and Wheat Gluten Moisture Content on Wheat Gluten Network Formation during Thermomolding. *J. Cereal Sci.* **2011**, *54*, 434–441.

(23) Jansens, K. J. A.; Vo Hong, N.; Telen, L.; Brijs, K.; Lagrain, B.; Van Vuure, A. W.; Van Acker, K.; Verpoest, I.; Van Puyvelde, P.; Goderis, B.; et al. Effect of Molding Conditions and Moisture Content on the Mechanical Properties of Compression Molded Glassy, Wheat Gluten Bioplastics. *Ind. Crops Prod.* **2013**, *44*, 480–487.

(24) Kontogiorgos, V. Microstructure of Hydrated Gluten Network. *Food Res. Int.* **2011**, *44*, 2582–2586.

(25) Rasheed, F.; Newson, W. R.; Plivelic, T. S.; Kuktaite, R.; Hedenqvist, M. S.; Gällstedt, M.; Johansson, E. Structural Architecture and Solubility of Native and Modified Gliadin and Glutenin Proteins: Non-Crystalline Molecular and Atomic Organization. *RSC Adv.* **2014**, *4*, 2051.

(26) Blomfeldt, T. O. J.; Kuktaite, R.; Johansson, E.; Hedenqvist, M. S. Mechanical Properties and Network Structure of Wheat Gluten Foams. *Biomacromolecules* **2011**, *12*, 1707–1715.

(27) Kuktaite, R.; Plivelic, T. S.; Türe, H.; Hedenqvist, M. S.; Gällstedt, M.; Marttila, S.; Johansson, E. Changes in the Hierarchical Protein Polymer Structure: Urea and Temperature Effects on Wheat Gluten Films. *RSC Adv.* **2012**, 11908–11914.

(28) Kuktaite, R.; Plivelic, T. S.; Cerenius, Y.; Hedenqvist, M. S.; Gällstedt, M.; Marttila, S.; Ignell, R.; Popineau, Y.; Tranquet, O.; Shewry, P. R.; et al. Structure and Morphology of Wheat Gluten Films: From Polymeric Protein Aggregates toward Superstructure Arrangements. *Biomacromolecules* **2011**, *12*, 1438–1448.

(29) Olabarrieta, I.; Cho, S.-W.; Gällstedt, M.; Sarasua, J.-R.; Johansson, E.; Hedenqvist, M. S. Aging Properties of Films of Plasticized Vital Wheat Gluten Cast from Acidic and Basic Solutions. *Biomacromolecules* **2006**, *7*, 1657–1664.

(30) Ullsten, N. H.; Cho, S.-W.; Spencer, G.; Gällstedt, M.; Johansson, E.; Hedenqvist, M. S.

Properties of Extruded Vital Wheat Gluten Sheets with Sodium Hydroxide and Salicylic Acid. *Biomacromolecules* **2009**, *10*, 479–488.

(31) Ullsten, N. H.; Gällstedt, M.; Johansson, E.; Gräslund, A.; Hedenqvist, M. S. Enlarged Processing Window of Plasticized Wheat Gluten Using Salicylic Acid. *Biomacromolecules* **2006**, *7*, 771–776.

(32) Türe, H.; Gällstedt, M.; Kuktaite, R.; Johansson, E.; Hedenqvist, M. S. Protein Network Structure and Properties of Wheat Gluten Extrudates Using a Novel Solvent-Free Approach with Urea as a Combined Denaturant and Plasticiser. *Soft Matter* **2011**, *7*, 9416.

(33) Kulasinski, K.; Guyer, R.; Keten, S.; Derome, D.; Carmeliet, J. Impact of Moisture Adsorption on Structure and Physical Properties of Amorphous Biopolymers. *Macromolecules* **2015**, 150408061558001.

(34) Henrik Ullsten, N.; Gällstedt, M.; Spencer, G. M.; Johansson, E.; Marttila, S.; Ignell, R.; Hedenqvist, M. S. Extruded High Quality Materials from Wheat Gluten. *Polym. from Renew. Resour.* **2010**, *1*, 173–186.

(35) Greenspan, L. Humidity Fixed Points of Binary Saturated Aqueous Solutions. *J. Res. Natl. Bur. Stand. Sect. A Phys. Chem.* **1977**, *81A*, 89.

(36) Santoro, G.; Yu, S.; Krywka, C.; Roth, S. V.; Ellis, G. Microfocus X-Ray Scattering and Micro-Raman Spectroscopy: Transcrystallinity in Isotactic Polypropylene. *Phys. status solidi - Rapid Res. Lett.* **2014**, *8*, 724–727.

(37) Buffet, A.; Rothkirch, A.; Döhrmann, R.; Körstgens, V.; Abul Kashem, M. M.; Perlich, J.; Herzog, G.; Schwartzkopf, M.; Gehrke, R.; Müller-Buschbaum, P.; et al. P03, the Microfocus and Nanofocus X-Ray Scattering (MiNaXS) Beamline of the PETRA III Storage Ring: The Microfocus Endstation. *J. Synchrotron Radiat.* **2012**, *19*, 647–653.

(38) Brüning, K.; Schneider, K.; Roth, S. V.; Heinrich, G. Kinetics of Strain-Induced Crystallization in Natural Rubber Studied by WAXD: Dynamic and Impact Tensile Experiments. *Macromolecules* **2012**, *45*, 7914–7919.

(39) Brüning, K. *In-Situ Structure Characterization of Elastomers during Deformation and Fracture*; Springer Theses; Springer International Publishing: Cham, 2014.

(40) Benecke, G.; Wagermaier, W.; Li, C.; Schwartzkopf, M.; Flucke, G.; Hoerth, R.; Zizak, I.; Burghammer, M.; Metwalli, E.; Müller-Buschbaum, P.; et al. A Customizable Software for Fast Reduction and Analysis of Large X-Ray Scattering Data Sets: Applications of the New DPDAK Package to Small-Angle X-Ray Scattering and Grazing-Incidence Small-Angle X-Ray Scattering. *J. Appl. Crystallogr.* **2014**, *47*, 1797–1803.

(41) Thomson, N. H.; Miles, M. J.; Popineau, Y.; Harries, J.; Shewry, P.; Tatham, A. S. Small Angle X-Ray Scattering of Wheat Seed-Storage Proteins: α-, γ- and ω-Gliadins and the High Molecular Weight (HMW) Subunits of Glutenin. *Biochim. Biophys. Acta - Protein Struct. Mol. Enzymol.* **1999**, *1430*, 359–366.

(42) Corporation, T. L. Distinguishing Amorphous Polymer Blends From Copolymers by Wide Angle X-Ray Diffraction. **1978**, *18*, 1144–1147.

(43) Bennion, B. J.; Daggett, V. The Molecular Basis for the Chemical Denaturation of Proteins by Urea. *Proc. Natl. Acad. Sci. U. S. A.* **2003**, *100*, 5142–5147.

(44) Mejri, M.; Rogé, B.; BenSouissi, A.; Michels, F.; Mathlouthi, M. Effects of Some Additives on Wheat Gluten Solubility: A Structural Approach. *Food Chem.* **2005**, *92*, 7–15.

(45) Maréchal, Y. Interaction Configurations of H2O Molecules in a Protein (Stratum Corneum) by Infrared Spectrometry. *J. Mol. Struct.* **1997**, *416*, 133–143.

(46) Ching, T. M.; Slabaugh, W. H. X-Ray Diffraction Analysis of Ice Crystals in Coniferous Pollen. *Cryobiology* **1966**, *2*, 321–327.

(47) Sterling, C. Gel-Water Relationships in Hydrophilic Polymers: X-Ray Diffraction of Fresh and Frozen Gels. *Cryobiology* **1969**, *5*, 393–397.

(48) Kishi, A.; Tanaka, M.; Mochizuki, A. Comparative Study on Water Structures in PolyHEMA and PolyMEA by XRD-DSC Simultaneous Measurement. *J. Appl. Polym. Sci.* **2009**, *111*, 476–481.

(49) Puzenko, A.; Hayashi, Y.; Feldman, Y. Space and Time Scaling in Glycerol-Water Mixtures. *J. Non. Cryst. Solids* **2007**, *353*, 4518–4522.

(50) Chadwell, H. M.; Politi, F. W. The Freezing Points of Concentrated Aqueous Solutions of Urea, Urethan, and Acetamide1. *J. Am. Chem. Soc.* **1938**, *60*, 1291–1293.

(51) Lane, L. B. Freezing Points of Glycerol and Its Aqueous Solutions. *Ind. Eng. Chem.* **1925**, *17*, 924.

(52) Kuktaite, R.; Plivelic, T. S.; Türe, H.; Hedenqvist, M. S.; Gällstedt, M.; Marttila, S.; Johansson, E. Changes in the Hierarchical Protein Polymer Structure: Urea and Temperature Effects on Wheat Gluten Films. *RSC Adv.* **2012**, *2*, 11908.

For Table of Contents Use Only

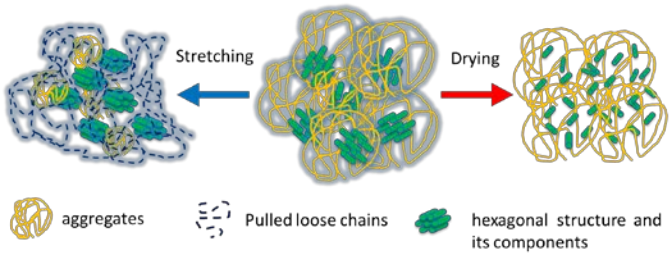

Moisture content and external loading modify the structure of wheat gluten plastics and are critical for reliable use of these in the sustainable society

The Structural Changes of Gluten/Glycerol Plastics at Dry and Moist Conditions and during Tensile Tests

Shun Yu, Fei Chen, Qiong Wu, Stephan Roth, Karsten Brüning, Konrad Schneider, Ramune Kuktaite,

Mikael Hedenqvist